Title Initial contact of glioblastoma cells with existing normal brain endothelial cells strengthen the barrier function via fibroblast growth factor 2 secretion: A new in vitro blood-brain barrier model.

Authors

Keisuke Toyoda ・ Kunihiko Tanaka ・ Shinsuke Nakagawa ・ Dinh Ha Duy Thuy ・ Kenta Ujifuku ・ Kensaku Kamada ・ Kentaro Hayashi ・ Takayuki Matsuo ・ Izumi Nagata ・ Masami Niwa

Affiliations

K. Toyoda ・ K. Ujifuku ・ K. Kamada ・ K. Hayashi ・ T. Matsuo ・ I. Nagata

Department of Neurosurgery, Nagasaki University Graduate School of Biomedical Sciences, 1-7-1 Sakamoto, Nagasaki 852-8501, Japan

K. Tanaka ・ S. Nakagawa ・ Thuy D. H. ・ M. Niwa

Department of Pharmacology, Nagasaki University Graduate School of Biomedical Sciences, 1-12-4 Sakamoto, Nagasaki 852-8523, Japan

S. Nakagawa ・ Thuy D. H. ・ M. Niwa

BBB Laboratory, PharmaCo-Cell Company Ltd., 1-43 Dejima, Nagasaki 850-0862, Japan

Running title Glioblastoma enhances blood-brain barrier by FGF-2

Corresponding Author

Kunihiko Tanaka, MD, PhD.

Department of Pharmacology, Nagasaki University Graduate School of Biomedical Sciences, 1-12-4 Sakamoto,

Nagasaki 852-8523, Japan

Phone: +81-95-819-7043, Fax: +81-95-819-7044

Email: kunny-ta@nagasaki-u.ac.jp

Abstract

Glioblastoma multiforme (GBM) cells invade along the existing normal capillaries in brain. Normal capillary endothelial cells function as the blood-brain barrier (BBB) that limits permeability of chemicals into the brain. To investigate whether GBM cells modulate the BBB function of normal endothelial cells, we developed a new *in vitro* BBB model with primary cultures of rat brain endothelial cells (RBECs), pericytes and astrocytes. Cells were plated on a membrane with 8 μm pores, either as a monolayer or as a BBB model with triple layer culture. The BBB model consisted with RBEC on the luminal side as a bottom, and pericytes and astrocytes on the abluminal side as a top of the chamber. Human GBM cell line, LN-18 cells, or lung cancer cell line, NCI-H1299 cells, placed on either the RBEC monolayer or the BBB model increased the transendothelial electrical resistance (TEER) values against the model, which peaked within 72 hours after the tumor cell application. The TEER value gradually returned to baseline with LN-18 cells, whereas the value quickly dropped to the baseline in 24 hours with NCI-H1299 cells. NCI-H1299 cells invaded into the RBEC layer through the membrane, but LN-18 cells did not. Fibroblast growth factor 2 (FGF-2) strengthens the endothelial cell BBB function by increased occludin and ZO-1 expression. In our model, LN-18 and NCI-H1299 cells secreted FGF-2, and a neutralization antibody to FGF-2 inhibited LN-18 cells-enhanced BBB function. These results suggest that FGF-2 would be a novel therapeutic target for GBM in the perivascular invasive front.

Key words

glioblastoma, blood-brain barrier, fibroblast growth factor 2, rat brain endothelial cells

Introduction

Glioblastoma multiforme (GBM) is one of the most malignant brain tumors. Despite optimal treatment and evolving standard care, median survival of the patients diagnosed with GBM is only 12-15 months (Wen et al. 2008). GBM cells tend to invade along certain preferred paths, particularly along existing normal blood vessels and fiber tracts in normal brain (Scherer 1940). In general, GBM tumor bulk is evaluated by contrast-enhanced radiography, and is surgically resected. However, GBM cells could remain in the peritumoral normal brain tissue even if all the radiographically-detectable tumor bulk has been resected. Since remnant GBM cells in the peritumoral tissue are one of the main sources for relapsing GBM, adjuvant chemoradiotherapy is indispensable, and new treatments targeting the perivascular invasion and/or its microenvironment where GBM cells invade and survive would be of additional benefit to improve survival from GBM.

Blood-brain barrier (BBB) is essential for maintenance of brain homeostasis by limiting permeability of foreign molecules to the brain. Major components of the BBB are brain microvascular endothelial cells that are closely interconnected via special cell-cell contacts, tight junctions (TJs) (Reese et al. 1967). Microvascular endothelial cells in brain also form dynamic interactions with other neighboring cells, such as astrocytes, pericytes, perivascular microglia and neurons, which form a neurovascular unit of the BBB (Dejana 2004). BBB provides ionic homeostasis and nutrients necessary for proper functioning of the central nervous system (CNS). BBB also protects

the nervous system from xenobiotics and regulates the level of neuroactive mediators (Paradridge 2002; Abbott 2005; Zlokovic 2008). In pathological conditions, however, limited permeability of the BBB hampers deliveries of drugs to the lesion. The BBB function of capillary endothelial cells in tumor bulk are disturbed (Nir et al. 1989), yet, it is not clear whether the GBM also disrupts the BBB function of normal capillaries, from which GBM cells invade in a normal brain.

Since 1973, several *in vitro* BBB models made with cultured cells have been developed (Deli 2007). In the BBB, TJs form a massive architecture with cell-cell adhesion molecules including membrane proteins, such as claudins, occludins and ZO-1, and are located between microvascular endothelial cells in the brain. TJs strictly restrict paracellular permeability. To assess functions of the TJs in an *in vitro* BBB model, measurement of the transendothelial electrical resistance (TEER) that reflects the junctional permeability for sodium ions, is one of the most straightforward methods (Deli et al. 2005). We recently reported a new *in vitro* BBB model, consisting with primary cultures of rat brain microvascular endothelial cells (RBECs), rat brain pericytes, and rat brain astrocytes, and showed that drug permeability in this model correlated with the BBB permeability *in vivo* (Nakagawa et al. 2009). However, the original model was designed with the luminal side as the top and the abluminal side as the bottom through a membrane with 0.4 μm pores. Here, we investigated direct interaction between glioblastoma cells and normal brain endothelial cells *in vitro*, using a modified BBB model, where abluminal side is on the top and luminal side is at the bottom through a membrane with 8 μm pores.

Using the modified *in vitro* BBB model with either monolayer or multilayer of brain cells, we investigated influence of GBM cells on the BBB function of normal brain endothelial cells, and compared with that of lung cancer cells. We found that GBM cells strengthen the barrier function of RBECs when the GBM cells form direct contact with basal side of the RBECs. In addition, GBM cells secreted fibroblast growth factor 2 (FGF-2) and enhanced the barrier function of RBECs by increasing expression of occludin and ZO-1 proteins in RBECs. These results suggest that our model is a useful tool for investigating interaction between the GBM cells and BBB, and that FGF-2 may play an important role for treating GBM at an invasive front.

Materials and Methods

Cell culture and Reagents

Wistar rats were obtained from Japan SLC, Inc., Japan. All animals were treated in strict accordance with the National Institutes of Health Guide for the Care and Use of Laboratory Animals (NIH Publications No. 80-23) and approved by Nagasaki University Animal Care Committee. Primary cultures of RBECs were prepared from 3-week-old rats, as previously described (Nakagawa et al. 2009; Deli et al. 1997; Nakagawa et al. 2007). Meninges were carefully removed from forebrains and gray matter was minced into small pieces of approximately 1 mm^3 in

ice-cold Dulbecco's modified Eagle's medium (DMEM), then dissociated by 25 strokes with a 5-ml pipette in DMEM containing collagenase type 2 (1 mg/ml, Worthington Biochemical Corp., USA), 300-µl DNase (15 µg/ml), gentamycin (50 µg/ml), and 2-mM glutamine. The resulting suspension was incubated on a shaker for 1.5 hours at 37°C, and the cells were pelleted by centrifugation (1000×g, 20 min) and re-suspended in 20% bovine serum albumin (BSA)-DMEM. The microvessels obtained in the pellet were further digested with collagenase-dispase (1 mg/ml, Roche Applied Sciences, Switzerland) and DNase (6.7 µg/ml in DMEM for 1 hour at 37°C). Microvascular endothelial cell clusters were separated on a 33% continuous Percoll (Pharmacia, Sweden) gradient, then collected and washed twice in DMEM before plating on 10 cm plastic dishes coated with collagen type IV and fibronectin (0.1 mg/ml each). RBEC cultures were maintained with DMEM/F12 supplemented with 10% plasma derived serum (PDS, Animal Technologies, Inc., USA), FGF-2 (1.5 ng/ml), heparin (100 µg/ml), insulin (5 µg/ml), transferrin (5 µg/ml), sodium selenite (5 ng/ml) (insulin-transferrin-sodium selenite media supplement), gentamycin (50 µg/ml), and puromycin (4 µg/ml) (RBEC medium I) at 37°C with a humidified atmosphere of 5% CO_2 /95% air for 2 days. According to the report by Perrière *et al*. (2005), we incubated cells for the first 2 days in medium containing puromycin (4 µg/ml) to avoid pericyte contamination. After 2 days, medium was switched with the RBEC medium II, which contained all the components of RBEC medium I except puromycin. When the cultures reached 80% confluency (4th days *in vitro*), the purified endothelial cells were passaged by brief treatment with trypsin (0.05%, w/v)-EDTA (0.02%, w/v) solution, and used for the *in vitro* models.

Rat brain astrocytes were obtained from neonatal Wistar rats. Meninges were removed and cortical pieces were mechanically dissociated in astrocyte culture medium (DMEM supplemented with 10% fetal bovine serum (FBS)), and then seeded in cell culture flasks. In order to obtain type 1 astrocytes, flasks with confluent cultures were shaken at 37°C overnight. Purity of the astrocytes was checked by the immunostaining for glial fibrillary acidic protein (GFAP), and the cells were used at passage 2 for subsequent experiments.

Pure cultures of rat brain pericytes were obtained by a 2-week culture of the isolated brain microvessel fragments, which were mixture of pericytes and endothelial cells. To isolate pericytes, the isolated microvessel fragments were cultured under a selective culture condition favoring pericyte survival and proliferation, using uncoated dishes, and DMEM supplemented with 10% FBS and antibiotics. Culture medium was changed every 3 days. Pericytes were characterized by their large size and branched morphology, positive immunostaining for α-smooth muscle actin, NG2 chondroitin sulfate proteoglycan and absence of von Willebrand factor and GFAP staining. Pericytes and astrocytes were frozen in cryo-medium Cellbanker (BCL-1, Zenoaq, Koriyama, Japan), and stored at -80°C until use.

Rat brain endothelial cell line GP8 (Greenwood et al. 1996) was kindly provided by Dr. Maria A. Deli. Human endothelial cell line HECV was purchased from Interlab Cell Line Collection (Genova, Italy). These cells were maintained in DMEM supplemented with 10% FBS and 100 μg/ml gentamycin.

Human glioblastoma cell line LN-18 and U-87 MG, and human non-small cell lung cancer cell line NCI-H1299 were purchased from American Type Culture Collection (Manassas, VA, USA). These cells were maintained in DMEM supplemented with 10% FBS, 500 unit/ml penicillin / 0.5 mg/ml streptomycin / 1.25 μg/ml amphotericin B, and 10% Mycokill AB (PAA Laboratories GmbH, Austria). G418 (0.5 mg/ml) was also added after transfection of green fluorescent protein (GFP)-expressing vector in LN-18 and NCI-H1299.

All the cells were grown in a humidified incubator at 5% CO_2 /95% air and 37°C, unless otherwise noted.

Reagents were purchased from Roche Applied Sciences, Switzerland (recombinant human fibroblast growth factor 2: FGF-2), from R & D Systems, Inc., USA (recombinant human vascular endothelial growth factor: VEGF and neutralization antibody against human FGF-2), and Sigma, USA for the other reagents, unless otherwise indicated.

Transfection of GFP-expressing vector for tumor cell lines

A GFP-expression vector, pAcGFP1-N1, was purchased from Clontech Laboratories, Inc., USA. The vector was transfected into LN-18 and NCI-H1299 cells using Lipofectamine™ 2000 (Invitrogen, USA) according to the manufacturer's instructions. Transfected cells were selected with 0.5 mg/ml G418 for 14 days and subcloned using cloning cylinders. After expression of the GFP was checked under a fluorescence microscope, the positive clones

were combined. GFP-expressing cells (LN-18-GFP cells and NCI-H1299-GFP cells) were used for the experiments within 10 passages.

Construction of models

***In vitro* monolayer models**

The day when GP8 cells, HECV cells, RBECs or pericytes/astrocytes were plated, or when BBB models were established was defined as Day zero. All models were made with a 24-well microtiter plate (Corning Incorporated Life Sciences, USA).

In vitro GP8, HECV, and RBEC monolayer models were generated by the following procedures. Cells were seeded at a density of 3×10^5 cells/cm^2 on the lower surface of a fibronectin-coated polyethylene terephthalate (PET) membrane with 8 μm pores in Millicell inserts (Millipore, USA) or a polycarbonate membrane with 0.4 μm pores in Transwell inserts (Corning Incorporated Life Sciences, USA), and cultured in the CO_2 incubator at 37°C for 3 hours. After the incubation, the monolayers were placed in a 24-well microtiter plate (Corning Incorporated Life Sciences, USA). The GP8 and HECV monolayers were maintained in DMEM supplemented with 10% FBS and 100 μg/ml gentamycin, and the RBEC monolayers were maintained in RBEC medium II supplemented with 500 nM hydrocortisone (Hoheisel et al. 1998) from Day 1.

***In vitro* pericytes/astrocytes co-cultured monolayer models and BBB models**

In vitro pericytes/astrocytes co-cultured monolayer model was constructed with pericytes (3×10^4 cells/cm^2) and astrocytes (2.7×10^5 cells/cm^2) seeded at a total density of 3×10^5 cells/cm^2 on the upper surface of the collagen type IV-coated PET membranes with 8 μm pores in Millicell inserts. The co-cultured monolayers were maintained in DMEM supplemented with 10% FBS and 100 μg/ml gentamycin.

Similarly, *in vitro* BBB model was constructed with RBECs seeded at a density of 3×10^5 cells/cm^2 on the lower surface of the fibronectin-coated PET membranes with 8 μm pores in Millicell inserts. The RBEC monolayers were incubated in the CO_2 incubator at 37°C for 3 hours, then maintained in a 24-well microtiter plate. Pericytes (3×10^4 cells/cm^2) and astrocytes (2.7×10^5 cells/cm^2) were then seeded at a total density of 3×10^5 cells/cm^2 on the upper surface of the membrane of the RBEC monolayers at Day 3. The *in vitro* BBB model was maintained in RBEC medium II, and supplemented with 500 nM hydrocortisone from Day 1.

Evaluation of the effect of tumor cells application on endothelial cells

Fluorescence microscopy

LN-18-GFP cells or NCI-H1299-GFP cells were placed at a density of 3×10^5 cells/cm^2 on the upper surface of either the *in vitro* monolayer models at Day 3, pericytes/astrocytes co-cultured monolayer models at Day 2, or *in vitro* BBB model at Day 5. Models with RBECs were used for subsequent analyses when absolute TEER values of the monolayer reached over 100 Ω × cm^2 at Day 3.

Tumor cell invasion to the endothelial cell layer at the lower surface of the membranes were assessed at Day 8 with the monolayer models using 24-well Millicell inserts and 8 μm pore-sized membranes. The upper surface of the membrane was wiped off carefully using cotton paper, and then the cells on the lower surface of the membrane were observed under a fluorescence microscopy (ECLIPSE E600, Nikon, Japan).

Transendothelial electrical resistance

TEER was measured by Epithelial-volt-ohm-meter (EVOM) and Endohm-6 (World Precision Instrument, USA). The extracellular matrix-coated inserts with or without tumor cells were measured as the background resistance, and TEER values of the models were corrected by subtracting the background values. TEER readings were also standardized for surface of the membrane and shown as absolute values ($\Omega \times cm^2$).

Effects of VEGF or FGF-2 on maintenance of the BBB function were evaluated as change of the TEER by recombinant human VEGF or FGF-2 added into the upper surface of the RBEC monolayers at Day 3 for 6 hours.

Western blot analysis

RBECs seeded at a density of 3×10^5 cells/cm^2 on the upper surface of a fibronectin-coated 12-well membrane in a Transwell inserts (Corning Incorporated Life Sciences, USA) were maintained with RBEC medium II supplemented with 500 nM hydrocortisone from Day 1, in the presence or absence of FGF-2 (1.5 ng/ml). When the RBECs without FGF-2 reached confluence (TEER values over 100 $\Omega \times cm^2$), cells in either conditions were harvested by scraping in CelLytic™ M cell lysis reagent supplemented with proteinase inhibitors (1 μg/ml aprotinin, 50 μg/ml

phenylmethylsulfonyl fluoride, and 1 μg/ml leupeptin). Lysates were centrifuged at 12,000 × g for 5 min at 4°C to collect supernatants as protein samples. Protein concentrations were determined with BCA protein assay reagent (Pierce, USA) and then the samples were heated in ×4 Laemmli sample buffer with β-mercaptoethanol at 95°C for 5 minutes. An equal amount of protein for each sample was separated by 12% SDS-PAGE and then transferred onto Hybond^{TM} –P (Amersham, UK). After blocking nonspecific binding sites with Perfect-Block (MoBiTec GmbH, Germany) (1% w/v) in Tris-buffered saline (25 mM Tris, 150 mM NaCl, 2 mM KCL, pH 7.4) containing 0.1% Tween-20 (TBS-T), blots were incubated with primary antibodies in the blocking solution for 1 hour at room temperature, followed by peroxidase-conjugated anti-mouse immunoglobulins (GE Healthcare, UK) as secondary antibodies. Anti-occludin and ZO-1 mouse monoclonal antibody (Invitrogen, USA) and anti-β-actin mouse monoclonal antibody were used in dilutions of 1:1,000, 1:2,500, and 1:5,000, respectively. Between the incubations, the blots were washed three times with TBS-T. The immunoreactive bands were visualized with SuperSignal West Femto Maximum Sensitivity Substrate (Pierce Biotechnology, USA), following the manufacturer`s instructions, and detected by FluorChem SP Imaging System (Alpha Innotech Corp., USA).

Enzyme-linked immunosorbent assays for FGF-2

Conditioned media were collected from tumor cells seeded at a density of 3.3×10^4 cells/cm^2 in 10 cm plastic dish with DMEM after 72 hours, and were cleared of cellular debris by 0.2 μm filter. The amounts of VEGF or FGF-2 in

the conditioned media were determined using Quantikine® Human VEGF or Human FGF basic enzyme-linked immunosorbent assay (ELISA) kits (R & D Systems, Inc., USA) following the manufacturer's instructions.

Neutralization of FGF-2 with anti-FGF-2 Antibody

Effects of FGF-2 derived from LN-18-GFP cells on the BBB function were assessed with a neutralization antibody to human FGF-2 (5 μg/ml) added into the upper surface of the *in vitro* RBEC monolayer models with or without tumor cells at Day 3, and the TEERs were measured after 6 hours.

Statistical analysis

Data are presented as the means ± standard error of mean (SEM) of at least three independent experiments. The values were compared using the analysis of variance followed by Student`s-t test or Tukey-Kramer test. Probability (p) value of less than 0.05 was considered to be statistically significant.

Results

Interaction between GBM cells and endothelial cells in *in vitro* models

Structure and the cellular constitutions of the monolayer and BBB models are shown in Fig. 1a. To investigate the interaction between the GBM cells and BBB, top chamber represents the abluminal side to apply tumor cells and the bottom chamber represents the luminal side lined with endothelial cells in our models. To evaluate the barrier function of the endothelial cells using our models, we first measured the TEERs of our models (Fig. 1b). The peak TEER values was significantly higher in RBEC monolayer and the BBB models (281.3 ± 14.6 Ω × cm^2, 329.4 ± 6.4 Ω × cm^2, respectively, $P < 0.01$ compared to the values in GP8- or HECV monolayer) than those in the GP8- or HECV monolayer models (9.5 ± 0.6 Ω × cm^2, and 53.2 ± 2.1 Ω × cm^2, respectively), indicating that only the RBEC monolayer and BBB model demonstrate adequate barrier function. Furthermore, the peak TEER values in the BBB model was significantly higher than that in the RBEC model ($P < 0.05$), suggesting that abluminal cells also play supportive role for endothelial-cell barrier function in the BBB.

GBM cells cannot intravasate into normal capillaries *in vivo* (Bernstein and Woodard 1995), therefore, our *in vitro* model was also designed to block the GBM cell invasion into the endothelial layer at the luminal side. First, we tested whether GBM cells can pass through the membrane used in our model without any cells layered. LN-18-GFP cells applied on the upper surface of the fibronectin-coated membrane with 0.4 μm pores were not detected at the lower surface of the membrane under a fluorescent microscope after 5 days, whereas cells on the 8 μm pore-sized membrane were observed (Fig. 2a). Then, we tested if LN-18-GFP cells pass through the endothelial cell layer underneath the membrane. As anticipated by design of the models, LN-18-GFP cells were observed on the lower

surfaces of the membranes of GP8 and HECV monolayers, but not at the lower surface of the membrane of RBEC monolayer (Fig. 2b). These results suggest that *in vitro* RBEC monolayer models reconstituted the brain capillary functions *in vivo* to block intravasation of the GBM cells into the brain capillaries.

Human GBM cells are known to impair the BBB functions (Grabb and Gilbert 1995; Ishihara et al. 2008). To further investigate a mechanism by which GBM cells affect the BBB function, we measured TEERs with LN-18-GFP cells applied in the upper chamber with the various endothelial cell monolayers and the BBB models. In the GP8 monolayer models (Fig. 3a, upper left), LN-18-GFP cells did not change the TEER values, presumably as GP8 monolayer model shows minimal the TEER values, hence does not form a functional BBB. In contrast, LN-18-GFP cells decreased the TEER values of HECV monolayer models (Fig. 3a, upper right) after 24 hours (53.2 ± 2.1 $\Omega \times cm^2$ vs. 27.4 ± 1.2 $\Omega \times cm^2$) and 48 hours (43.0 ± 2.1 $\Omega \times cm^2$ vs. 12.9 ± 1.1 $\Omega \times cm^2$). LN-18-GFP cells also decreased the TEER values of RBEC monolayer models with the 0.4 μm pore-sized membranes (Fig. 3a, lower left) after 24 hours (125.9 ± 3.1 $\Omega \times cm^2$ vs. 94.3 ± 2.8 $\Omega \times cm^2$) and 48 hours (200.0 ± 6.2 $\Omega \times cm^2$ vs. 108.6 ± 6.4 $\Omega \times cm^2$). In contrast, LN-18-GFP cells significantly increased the TEER values of *in vitro* RBEC monolayer models with the 8 μm pore-sized membranes (Fig. 3a, lower right) after 24 hours (141.3 ± 5.8 $\Omega \times cm^2$ vs. 202.6 ± 5.9 $\Omega \times cm^2$) and 48 hours (226.0 ± 8.5 $\Omega \times cm^2$ vs. 324.4 ± 12.3 $\Omega \times cm^2$). Interestingly, when LN-18-GFP cells were in direct contact with the apical side of the RBECs, GBM cells decreased the TEER values of an *in vitro* BBB

model, in which the RBECs were located on the upper-, and pericytes/astrocytes on the lower surface of the membrane (data not shown).

To investigate whether GBM cells also strengthen the BBB function under the environment more similar to *in vivo* conditions, we next utilized the *in vitro* BBB models that were made with RBECs, pericytes and astrocytes. LN-18-GFP cells applied to the upper chamber significantly increased the TEER values of the *in vitro* BBB models after 48 hours (Fig. 3b, upper panel; $319.4 \pm 9.2\ \Omega \times cm^2$ vs. $400.3 \pm 12.8\ \Omega \times cm^2$). The LN-18-GFP cells were not observed on the lower surface of the membrane even after 10 days from their application (Fig. 3b, lower left), whereas the cells invaded on to the lower surface of the membrane even after 2 days when applied on to an *in vitro* pericytes/astrocytes co-cultured monolayer without RBEC at the lower surface (Fig. 3b, lower right). These results suggest that GBM cells strengthen the barrier function of brain endothelial cells, specifically when GBM cells directly contact with the basal side of the RBECs even in *in vitro* model of the BBB.

Effects of FGF-2 on the BBB function in *in vitro* RBEC monolayer model

Next, we tested if only GBM cells can strengthen the BBB function, by comparing with the effects of a lung cancer cell line, NCI-H1299-GFP cells (Fig. 4). *In vivo*, NCI-H1299 cells could metastasize to brain (Huang et al. 2002). NCI-H1299 cells also increased the TEER values of RBEC monolayer models and significantly more so compared with that of LN-18-GFP cells at 24 hours after their application ($308.0 \pm 5.4\ \Omega \times cm^2$ vs. $202.6 \pm 5.9\ \Omega \times cm^2$).

Interestingly, the TEER values peaked with NCI-H1299-GFP cells quickly dropped to the basal levels within 24 hours and the cells were observed on the lower surface of the membrane after 5 days from their application on to the model. On the other hand, with LN-18-GFP cells, the TEER values returned to the basal levels only gradually and the GBM cells were never detected on the lower surface of the membrane. These results suggest that, though both GBM and lung cancer cells could temporarily strengthen the BBB function of the RBECs, only GBM cells have prolonged strengthening effects on the BBB function, whereas lung cancer cells rather disrupt the tight junction and invade into the endothelial cell layer.

Since both LN-18-GFP cells and NCI-H1299-GFP cells increased the TEER values of *in vitro* RBEC monolayer models in the early stage when these cells directly contacted with the basal side of the RBECs, we hypothesized that the effects on the BBB might be mediated by a growth factor secreted by LN-18 cells and NCI-H1299 cells. VEGF is one of the well-known angiogenesis factors in GBM. On the other hand, FGF-2 is one of the growth factors that could strengthen the BBB function *in vitro* and *in vivo* (Bendfeldt et al. 2007; Reuss et al. 2003), and GBM cells could secrete FGF-2 for their own growth and/or invasion (Okumura et al. 1989; Lund-Johansen et al. 1992). We measured VEGF and FGF-2 levels in the conditioned media of either LN-18 cells or NCI-H1299 cells by ELISA. Indeed, both cell lines produced VEGF and FGF-2, and another GBM cells, U-87 MG, also increased both VEGF and FGF-2 levels (Table 1).

Since GBM and lung cancer cells temporarily strengthened the BBB function of the RBECs, and both cell lines secrete VEGF and FGF-2, we next tested if exogenous VEGF or FGF-2 strengthens the BBB function of RBEC monolayer models. In confluent monolayer of RBECs that showed TEER values over 100 $\Omega \times cm^2$, exogenous VEGF decreased the TEER values after 6 hours (100.0 ± 0.4%, 75.4 ± 1.3%, 70.1 ± 2.5%, 68.5 ± 1.5% for 0, 10, 50, 100 ng/ml of VEGF, respectively, Fig. 5a left), while FGF-2 increased the TEER values after 6 hours (100.0 ± 1.2%, 114.3 ± 1.8%, 126.2 ± 1.2%, 134.3 ± 1.2% for 0, 0.5, 1.0, 1.5 ng/ml of FGF-2, respectively, Fig. 5a right). FGF-2 treatment also increased expressions of TJ proteins, occludin and ZO-1 in the RBEC monolayer (Fig. 5b), implying that FGF-2 strengthen the BBB function of the RBECs by regulating the expressions of occludin and ZO-1 proteins. Subsequently, we tested if FGF-2 derived from LN-18-GFP cells mediates to strengthen BBB function of the RBECs. Incubation of the LN-18-GFP cells with a neutralizing antibody against human FGF-2 added into the upper chamber of the RBEC monolayer models, inhibited the increase of TEERs measured 6 hours after tumor cell application (100.0 ± 2.5% vs. 80.5 ± 0.2%, Fig. 6 right), whereas the TEER values without tumor cell application were not affected (Fig. 6 left). These results suggested that FGF-2 secreted by GBM cells plays a pivotal role in strengthening the BBB function of the RBECs when GBM cells make initial direct contact with the basal side of the RBECs.

Discussion

In the present study, we investigated, using a newly-constructed *in vitro* model, if GBM cells affect the BBB function of normal microvessels, through which GBM cells invade. RBEC monolayers, but not the other endothelial cell lines, seeded on the lower surface of the membrane demonstrated sufficient BBB function. The co-culture system of cerebral pericytes and astrocytes on the upper surface of the 8 μm pore-sized membrane provided direct contact of tumor cells with the basal side of primary endothelial cells. Several *in vitro* co-culture models using the human GBM cells and the endothelial cells were previously reported (Grabb and Gilbert 1995; Ishihara et al. 2008). Those models were constructed with endothelial cells seeded on the upper surface, and human GBM cells seeded at the bottom in the plate enabling those models mainly to assess effects of soluble factors derived from the human GBM cells on the endothelial cells. On the other hand, our *in vitro* model resembles more to an organic BBB environment, and assesses effects of GBM cells directly contacting with the basal side of the primary endothelial cells. Therefore, our model uniquely mimics the early encounter of the GBM cells, which an *in vivo* model cannot demonstrate. Using this novel system constructed with primary rat brain microvascular endothelial cells, we found that LN-18 cells, as a model of human GBM cells, strengthen the BBB function of RBECs.

Many factors modulate the BBB function and angiogenesis in a brain. For example, VEGF, tumor necrosis factor-α (TNF-α), transforming growth factor-β (TGF-β) and matrix-metalloproteinases (MMPs) could attenuate (Argaw et al. 2009; Dobbie et al. 1999; Behzadian et al. 2001; Yang and Rosenberg 2011), whereas FGF-2 could

strengthen the BBB function (Bendfeldt et al. 2007; Reuss et al. 2003). In mouse that lacks FGF-2, expression of tight junction proteins, such occludin and ZO-1, was decreased (Reuss et al. 2003). Conversely, in our *in vitro* model, exogenous FGF-2 enhanced the BBB function of the RBECs. Since very few factors were known to strengthen the BBB function of the endothelial cells, we hypothesized that GBM cells secret FGF-2 and strengthen the BBB function in our *in vitro* model. Indeed, conditioned media of either LN-18 or NCI-H1299 cells contained FGF-2, and a neutralization antibody to FGF-2 abrogated the increase of TEER by LN-18 cells. GBM cells express both enhancing factors, such as FGF-2 (Okumura et al. 1989; Lund-Johansen et al. 1992), and attenuating factors, such as VEGF, TGF-β, and MMPs (Plate et al 1992; Dunn et al. 2000; Yamamoto et al. 1998) of the BBB function. Interestingly, the BBB function was rather attenuated when GBM cells directly contacted with the apical side of the endothelial cells. Based on the present results with our RBEC monolayer models and reports from others (Grabb and Gilbert 1995; Ishihara et al. 2008), it appears that attenuating effects on the BBB function are dominant when GBM cells contact with the basal side of the endothelial cells indirectly through the 0.4 μm pore-sized membranes, whereas the enhancing effects become dominant when GBM cells contacted with the basal side of the endothelial cells directly through the 8 μm pore-sized membranes. FGF-2 production by astrocytes that are in close proximity to endothelial cells of the BBB is also reported (Sobue et al. 1999). FGF-2 exhibits a wide range of angiotrophic effects, and activates signaling pathways regulating endothelial cell survival (Sobue et al. 1999; Klint et al. 1999), via activation of FGF receptor 1 (FGFR1) on the endothelial cells (Klint et al. 1999), presumably at the basal side of the

endothelial cells (Tanghetti et al. 2002). It is intriguing that secreted FGF2 appeared effective only when GBM cells are in direct contact with the endothelial cells. We speculated the following potential explanations for this finding; 1, a molecule expressed at the basal side of the endothelial cells is required for the GBM cells to secrete FGF2 , 2, GBM cells secrete FGF2 regardless of their approach, apical or basal, to endothelial cells, but, but FGF2 cannot bind to its receptor expressed preferentially at the basal side of endothelial cells, for either the secreted FGF2 from the apical side cannot pass tight junction, or FGF2 is quickly degraded before reaching to the receptor at basal side of endothelial cells when FGF2 is released from the apical side. Endothelial cells themselves might also strengthen the BBB function when they are in direct contact with the GBM cells as a protective mechanism. Furthermore, GBM cells can proteolytically release FGF-2, which normally is present in most of the GBM tumor as a bound form to the extracellular matrix surrounding the proliferating blood vessels (Stefaik et al. 1991), when the cells were directly attached to the basement membrane of the endothelial cells. GBM cells are directly attached to the existing brain capillaries at the initial stage. As the tumor progress, the geography changes and subsequent angiogenesis occurs (Winkler et al. 2009). The neovascular structure lacks the BBB function and becomes dominant at the advanced stage of angiogenesis, as evidenced by peritumoral edema and enhanced image of tumor bulk by a radiographical evaluation. Therefore, our findings demonstrate a pivotal early event where the BBB function is rather strengthened at initial contact of the GBM cells with existing capillaries. The functional meanings of this first response are not clear at this point but warrant further evaluation. It was intriguing that a lung cancer cell line, NCI-H1299, also

showed transient increase of TEER values with the RBEC monolayer model. Since both cell lines secret FGF-2 in culture, the putative role for FGF-2 in mediating the transient strengthening of the BBB function at the initial contact might be universal in at least these two tumor cell lines tested in the present study. Conversely, subsequent events differ in the two cell lines. With lung cancer cells, the TEER values quickly returned to the baseline and the monolayer became permeable, whereas the values were rather sustained and gradually decreased with GBM cells. The difference may reflect physiological characteristics of these two different cell types or their origins.

With magnetic resonance imaging (MRI), gadolinium-enhanced T1-weighted image (T1WI) shows tumor bulk of GBM, surrounded by hyper-intensity area of T2-weighted image (T2WI) indicates brain edema, caused by disrupted BBB. Thus, in areas next to the tumor bulk and visualized as normal on T2WI, the BBB function must be relatively intact. However, histological examination revealed that the tumor cells are spread beyond the borders of the hyper-intensity areas shown on T2WI (Watanabe et al. 1992; Tovi et al 1994). Since micro-invasion of GBM cells cannot be visualized with current imaging techniques, tumor bulk of GBM is in general surgically resected including the area with hyper-intensity on T2WI-weighed images, followed by postoperative irradiation and/or chemotherapy. Interaction of GBM cells with the existing capillaries induces angiogenesis consisting with endothelial cells that lack appropriate functions, resulting in decreased BBB function (ZagZag et al. 1989). Data from the present study suggest that the BBB function is rather temporarily strengthened in a close vicinity of the tumor bulk, as visualized with normal T2WI area, where GBM cells make first contact with the existing, relatively normal capillary

endothelial cells and where angiogenesis has not yet become apparent. In 1990s, a new drug temozolomide (TMZ) was introduced (Plowman et al. 1994). TMZ chemotherapy in combination with radiotherapy demonstrated statistically significant prognostic advantage in GBM patients, and thus has become the first line chemoradiotherapy regimen for treatment of GBM (Stupp et al. 2005). However, long-term outcome analyses showed that addition of TMZ to radiotherapy only minimally prolongs median survival time in newly diagnosed GBM patients, such as 14.6 versus 12.1 months, and the best 5-year survival of 9.8% (Stupp et al. 2009). TMZ is reasonably detected in cerebrospinal fluid (CSF) (Ostermann et al. 2004). Drug concentration in CSF is often used as a surrogate for assessing drug delivery to brain tissue or in extra-cellular fluid. However, accuracy of this approximation is limited as barrier functions of the BBB and blood-CSF barrier are remarkably different (de Lange and Danhof 2002). *In vivo* studies showed TMZ delivery into the tumor bulk through blood vessels, in which the BBB function was weakened (Kato et al. 2010). However, it was not clear whether TMZ is also delivered to the area visualized as normal by radiographical assessment. Furthermore, the tissue concentration of TMZ was quite low in high-grade glioma (Pitz et al. 2011). Therefore, permeability of drugs, such as TMZ, into the areas of GBM cells invasive front could be limited, if GBM cells in the areas visualized as normal on T2WI had tighten the BBB function of normal capillaries, as indicated in this study. Therefore, treatment strategy targeting GBM cells, such as neutralizing FGF-2, at invasive front may prolong survival of patients with GBM.

GBM cells increased the barrier function of the RBECs in a novel *in vitro* BBB model, when GBM cells directly contacted with the basal side of the RBECs, without invading into the RBEC layer. FGF-2 derived from GBM cells were implicated in these effects. Recently, possible role for interaction between GBM cells and brain capillaries has also been suggested in formation of vascular niche (Gilbertson and Rich 2007), in addition to the roles in tumor cell invasion along capillaries and angiogenesis. Together, FGF-2 may contribute to the first step of GBM invasion along capillaries, angiogenesis, and niche formation in normal brain tissue, all of which may cause drug resistance in the perivascular invasive front of GBM cells. Therefore, results from the present study suggest that FGF-2 is a key molecule for GBM treatment in the invasive front.

Acknowledgments

We thank Ms. Mayumi Sagara of the BBB Laboratory, PharmaCo-Cell Company Ltd., and Mr. Ken Izawa and Mr. Daisuke Watanabe of the Sano Drug Group for their contributions. This work was supported in part by Grant-in-Aid for Scientific Research (#23592094 to K.H. and #23592095 to K.U.) from Ministry of Education, Culture, Sports, Science and Technology of Japan.

Conflict of interest

We have nothing to disclose in terms of financial support or relationships that may pose a conflict of interest.

References

Abbott NJ (2005) Dynamics of CNS barriers: evolution, differentiation, and modulation. Cell Mol Neurobiol 25:5-23

Argaw AT, Gurfein BT, Zhang Y, Zameer A, John GR (2009) VEGF-mediated disruption of endothelial CLN-5 promotes blood-brain barrier breakdown. Proc Natl Acad Sci USA 106:1977-1982

Behzadian MA, Wang XL, Windsor LJ, Ghaly N, Caldwell RB (2001) TGF-beta increases retinal endothelial cell permeability by increasing MMP-9: Possible role of glial cells in endothelial barrier function. Invest Ophthalmol Vis Sci 42:853-859

Bendfeldt K, Radojevic V, Kapfhammer J, Nitsch C (2007) Basic fibroblast growth factor modulates density of blood vessels and preserves tight junctions in organotypic cortical cultures of mice: A new *in vitro* model of the blood-brain barrier. J Neurosci 27:3260-3267

Bernstein JJ, Woodard CA (1995) Glioblastoma cells do not invasate into blood vessels. Neurosurgery 36:124-132

de Lange EC, Danhof M (2002) Considerations in the use of cerebrospinal fluid pharmacokinetics to predict brain target concentrations in the clinical setting: implications of the barriers between blood and brain. Clin Pharmacokinet 41:691-703

Dejana E (2004) Endothelial cell-cell junctions: Happy together. Nat Rev Mol Cell Biol 5:261-270

Deli MA, Szabo C, Dung N, Joo F (1997) Immunohistochemical and electron microscopy detections on primary cultures of rat cerebral endothelial cells. In: Boer AG, Sutant W (eds) Drug transport across the blood-brain barrier: In vivo and in vitro techniques. Harwood Academic Publishers, Amsterdam:23-28

Deli MA, Ábrahám CS, Kataoka Y, Niwa M (2005) Permeability studies on in vitro blood-brain barrier models: physiology, pathology and pharmacology. Cell Mol Neurobiol 25:59-127

Deli MA (2007) Blood-brain barrier models. In: Lajtha, A. (Ed.), Handbook of Neurochemistry and Molecular Neurobiology, Neural Membranes and Transport, vol. 11. Springer, NewYork:29-56

Dobbie MS, Hurst RD, Klein NJ, Surtees RA (1999) Upregulation of intracellular adhesion molecule-1 expression on human endothelial cells by tumour necrosis factor-α in an in vitro model of the blood-brain barrier. Brain Res 830:330-336

Dunn IF, Hesse O, Black P (2000) Growth factors in glioma angiogenesis: FGFs, PDGF, EGF, and TGFs. J Neurooncol 50:121-137

Gilbertson RJ, Rich JN (2007) Making a tumour`s bed: glioblastoma stem cells and the vascular niche. Nat Rev Cancer 7:733-736

Grabb PA, Gilbert MR (1995) Neoplastic and pharmacological influence on the permeability of an *in vitro* blood-brain barrier. J Neurosurg 82:1053-1058

Greenwood J, Pryce G, Devine L, Male DK, dos Santos WL, Calder VL, Adamson P (1996) SV40 large T immortalized cell lines of the rat blood-brain and blood-retinal barriers retain their phenotypic and immunological characteristics. J Neuroimmunol 71:51-63

Hoheisel D, Nitz T, Franke H, Wegener J, Hakvoort A, Tilling T, Galla H-J (1998) Hydrocortisone reinforces the blood-brain barrier properties in a serum free cell culture system. Biochem Biophys Res Commun 247:312-315

Huang MS, Wang TJ, Liang CL, Huang HM, Yang IC, Yi-Jan H, Hisao M (2002) Establishment of fluorescent lung carcinoma metastasis model and its real-time microscopic detection in SCID mice. Clin Exp Metastasis 19:359-368

Ishihara H, Kubota H, Lindberg RL, Leppert D, Gloor SM, Errede M, Virgintino D, Fontana A, Yonekawa Y, Frei K (2008) Endothelial cell barrier impairment induced by glioblastomas and transforming growth factor β_2 involves matrix metalloproteinase and tight junction proteins. J Neuropathol Exp neurol 67:435-448

Kato Y, Holm DA, Okollie B, Artemov D (2010) Noninvasive detection of temozolomide in brain tumor xenografts by magnetic resonance spectroscopy. Neuro Oncol 12:71-79

Klint P, Kanda S, Kloog Y, Claesson-Welsh L (1999) Contribution of Src and Ras pathways in FGF-2 induced endothelial cell differentiation. Oncogene 18:3354-3364

Lund-Johansen M, Forsberg K, Bjerkvig R, Laerum OD (1992) Effects of growth factors on a human glioma cell line during invasion into rat brain aggregates in culture. Acta Neuropathol 84:190-197

Nakagawa S, Deli MA, Nakao S, Honda M, Hayashi K, Nakaoke R, Kataoka Y, Niwa M (2007) Pericytes from brain microvessels strenghthen the barrier integrity in primary cultures of rat brain endothelial cells. Cell Mol Neurobiol 27:687-694

Nakagawa S, Deli MA, Kawaguchi H, Shimizudani T, Shimono T, Kittel A, Tanaka K, Niwa M (2009) A new blood-brain barrier model using primary rat brain endothelial cells, pericytes and astrocytes. Neurochem Int 54:253-263

Nir I, Levanon D, Iosilevsky G (1989) Permeability of blood vessels in experimental gliomas: Uptake of 99mTc-glucoheptonate and alteration in blood-brain barrier as determined by cytochemistry and electron microscopy. Neurosurgery 25:523-531

Okumura N, Takimoto K, Okada M, Nakagawa H (1989) C6 glioma cells produce basic fibroblast growth factor that can stimulate their own proliferation. Biochemistry 106:904-909

Ostermann S, Csajka C, Buclin T, Leyvraz S, Lejeune F, Decosterd LA, Stupp R (2004) Plasma and cerebrospinal fluid population pharmacokinetics of temozolomide in malignant glioma patients. Clin Cancer Res 10:3728-3736

Paradridge WM (2002) Drug and gene targeting to brain with molecular Trojan horses. Nat Rev Drug Discove 1:131-139

Perrière N, Demeuse P, Garcia E, Regina A, Debray M, Andreux JP, Couvreur P, Scherrmann JM, Temsamani J, Couraud PO, Deli MA, Roux F (2005) Puromycin-based purification of rat brain capillary endothelial cell cultures. Effect on the expression of blood-brain barrier-specific properties. J Neurochem 93:279-289

Pitz MW, Desai A, Grossman SA, Blakeley JO (2011) Tissue concentration of systemically administered antineoplastic agents in human brain tumors. J Neurooncol 104:629-638

Plate KH, Breier G, Weich HA, Risau W (1992) Vascular endothelial growth factor is a potential tumor angiogenesis factor in human gliomas in vivo. Nature 359:845-848

Plowman J, Waud WR, Koutsoukos AD, Rubinstein LV, Moore TD, Grever MR (1994) Preclinical antitumor activity of temozolomide in mice: efficacy against human brain tumor xenografts and synergism with 1,3-bis(2-chloroethyl)-1-nitrosourea. Cancer Res 54:3793-3799

Reese TS, Karnovsky MJ (1967) Fine structural location of a blood-brain barrier to exogenous peroxidase. J Cell Biol 34:207-217

Reuss B, Dono R, Unsicker K (2003) Functions of fibroblast growth factor (FGF)-2 and FGF-5 in astroglial differentiation and blood-brain barrier permeability: evidence from mouse mutants. J Neurosci 23:6404-6412

Scherer HD (1940) Cerebral astrocytomas and their derivatives. Am J Cancer 1:159-198

Sobue K, Yamamoto N, Yoneda K, Hodgson ME, Yamashiro K, Tsuruoka N, Katsuya H, Miura Y, Asai K, Kato T (1999) Induction of blood brain barrier properties in immortalized bovine brain endothelial cells by astrocytic factors. Neurosci Res 35:155-164

Stefaik DF, Rizlkalla LR, Soi A, Goldblatt SA, Rizkalla WM (1991) Acidic and basic fibroblast growth factors are present in glioblastoma multiforme. Cancer Res 51:5760-5705

Stupp R, Mason WP, van den Bent MJ, Weller M, Fisher B, Taphoorn MJ, Belanger K, Brandes AA, Marosi C, Bogdahn U, Curschmann J, Janzer RC, Ludwin SK, Gorlia T, Allgeier A, Lacombe D, Cairncross JG, Eisenhauer E, Mirimanoff RO (2005) Radiotherapy plus concomitant and adjuvant temozolomide for glioblastoma. N Engl J Med 352:987-996

Stupp R, Hegi ME, Mason WP, van den Bent MJ, Taphoorn MJ, Janzer RC, Ludwin SK, Allgeier A, Fisher B, Belanger K, Hau P, Brandes AA, Gijtenbeek J, Marosi C, Vecht CJ, Mokhtari K, Wesseling P, Villa S, Eisenhauer E, Gorlia T, Weller M, Lacombe D, Cairncross JG, Mirimanoff RO (2009) Effects of radiotherapy with concomitant and adjuvant temozolomide versus radiotherapy alone on survival in glioblastoma in a randomised phase III study: 5-year analysis of the EORTC-NCIC trial. Lancet Oncol 10:459-466

Tanghetti E, Ria R, Dell`Era P, Urbinati C, Rusnati M, Ennas MG, Presta M (2002) Biological activity of substrate-bound basic fibroblast growth factor (FGF2): recruitment of FGF receptor-1 in endothelial cell adhesion contacts. Oncogene 21:3889-3897

Tovi M, Hartman M, Lilja A, Ericsson A (1994) MR imaging in cerebral gliomas. Tissue component analysis in correlation with histopathology of whole-brain specimens. Acta Radiol 35:495-505

Watanabe M, Tanaka R, Taeda N (1992) Magnetic resonance imaging and histopathology of cerebral gliomas. Neuroradiology 34:463-469

Wen PY, Kesari S (2008) Malignant gliomas in adults. N Engl J Med 359:492-507

Winkler F, Kienast Y, Fuhrmann M, Von Baumgarten L, Burgold S, Mitteregger G, Kretzschimar H, Herms J (2009) Imaging glioma cell invasion in vivo reveals mechanisms of dissemination and peritumoral angiogenesis. Glia 57:1306-1315

Yamamoto M, Mohanam S, Sawaya R (1998) Differential expression of membrane-type matrix metalloproteinase and its correlation with gelatinase A activation in human malignant brain tumors in vivo and in vitro. Cancer Res 56:384-92

Yang Y, Rosenberg GA (2011) MMP-mediated disruption of claudin-5 in the blood-brain barrier of rat brain after cerebral ischemia. Methods Mol Biol 762:333-345

ZagZag D, Goldenberg M, Brem S (1989) Angiogenesis and blood-brain barrier breakdown modulate CT contrast enhancement: an experimental study in a rabbit brain-tumor model. Am J Roentgenol 153:141-146

Zlokovic BV (2008) The blood-brain barrier in health and neurodegenerative disorders. Neuron 57:178-201

Figure Legends

Fig. 1: The schemas of the *in vitro* models, and the peak TEER values in each model.

a *In vitro* monolayer models were constructed by seeding various endothelial cells on the lower side of the 8 μm pore-sized membranes, and *in vitro* BBB models were constructed by seeding pericytes and astrocytes on the upper side of 8 μm pore-sized membrane, and RBECs on the lower side of the membrane.

b Each model was constructed as described in Materials and Methods. The TEERs were measured every day from Day 2. The peak TEER value of each model was shown as $\Omega \times cm^2$. Data are presented as the mean ± SEM of three independent experiments. $*P < 0.05$ and $**P < 0.01$, between the two groups indicated by Tukey-Kramer test.

Fig. 2: Transmigration of LN-18-GFP cells through a membrane with endothelial monolayer.

a LN-18-GFP cells were applied on the upper surface of a fibronectin-coated membrane with either 0.4- or 8 μm pores. After 5 days, the cells on the upper surface of the membrane were wiped off and the lower surface of the membrane was observed under a fluorescence microscopy.

b LN-18-GFP cells were applied on the upper surface of the *in vitro* monolayer models made with various endothelial cells on the lower surface of the 8 μm pore-sized membranes at Day 3. After 5 days, the cells on the upper surface of the membrane were wiped, and the lower surface of the membrane was observed under a fluorescence microscopy.

Fig. 3: The TEER values of LN-18-GFP cells in the RBEC monolayer models or the BBB models.

a TEER values of the monolayer models. LN-18-GFP cells were applied in the upper chamber of the models at Day 3, and the TEERs were measured 0, 24, and 48 hours after application of the cells.

b TEER values of the BBB models. LN-18-GFP cells were applied on the upper surface of the models at Day 5, and the TEERs were measured 0, 24, and 48 hours after application of the cells (upper panel). The TEER value of the models without application of the LN-18-GFP cells is shown as control. Results are shown as the mean ± SEM of three independent assays. $^{**}P < 0.01$, compared to the control. LN-18-GFP cells were applied in the upper chamber of either the BBB model at Day 5 or to the pericytes/astrocytes monolayer without RBECs at Day 2. The cells on the lower surface of the membrane were observed under a fluorescence microscope either 48 hours or 10 days after the GBM cells application, in pericytes/astrocytes monolayer or the BBB models, respectively (lower panels).

Fig. 4: The TEER values and transmigration of the RBEC monolayer models with LN-18-GFP or NCI-H1299-GFP cells.

LN-18-GFP cells or NCI-H1299-GFP cells were applied on the upper surface of the RBEC models with the 8 μm pore-sized membrane at Day 3, and the TEERs were measured daily up to Day 13 for the models with LN-18 and control, and up to Day 8 for the models with NCI-H1299 cells (upper panel). Control TEER values were measured

with the models without the tumor cells application. Results are shown as the mean ± SEM of three independent assays. *$P < 0.01$, compared to the control. **$P < 0.01$, compared to the values with LN-18. At Day 8, NCI-H1299-GFP cells migrated on to the lower surface of the RBEC monolayer models were observed under a fluorescence microscope, but LN-18-GFP cells were not (lower panels).

Fig. 5: Effects of VEGF or FGF-2 on the BBB function and TJ protein expression.

a The RBEC monolayer models were constructed with 8 μm pore-sized membrane. At Day 3 when the TEERs reached over 100 Ω × cm^2, different concentrations of VEGF (0, 10, 50, and 100 ng/ml) or FGF-2 (0, 0.5, 1.0, and 1.5 ng/ml) were added to the upper chamber of the models, and the TEERs were measured after 6 hours. The TEER values are expressed as a percent of the value in the models without VEGF (100% = 101.6 ± 0.4 Ω × cm^2) or FGF-2 after 6 hours (100% = 101.6 ± 1.2 Ω × cm^2). Results are shown as the mean ± SEM of three independent assays. *$P < 0.05$, **$P < 0.01$, compared by ANOVA among the groups with VEGF or FGF-2 different concentrations.

b Expressions of tight junction protein, occludin and ZO-1, in the *in vitro* RBEC monolayer models. RBECs were seeded on fibronectin-coated 12-well Transwell inserts with or without 1.5 ng/ml FGF-2. RBECs of the models were harvested when the models without FGF-2 reached confluence (TEER values over 100 Ω × cm^2), and the lysates were subjected to Western blot analysis with specific antibodies of occludin and ZO-1. β-actin was used as an internal control (left panels). Expressions of occludin and ZO-1 proteins were densitometrically evaluated after

collection for the β-actin levels (right panel). Results are shown as the mean ± SEM of three independent assays. *P < 0.05, compared to FGF-2 (-).

Fig. 6: TEER values of the RBEC monolayer models with a neutralization antibody against FGF-2.

A neutralization antibody against human FGF-2 was added in the upper chamber of the RBEC models Day 3 and the TEERs were measured after 6 hours. The TEER values are shown as a percent change from either those of the control models without antibody (left panel. 100% = 112.0 ± 2.3 Ω × cm^2 left) or those of the models with LN-18-GFP cells (right panel. 100% = 108.0 ± 2.7 Ω × cm^2, right). Results are shown as the mean ± SEM of three independent assays. Gray bars; controls, black bars; with addition of anti-FGF-2 antibody. **P < 0.01, compared to the values with LN-18 in the absence of the neutralizing antibody.

Fig. 1

A

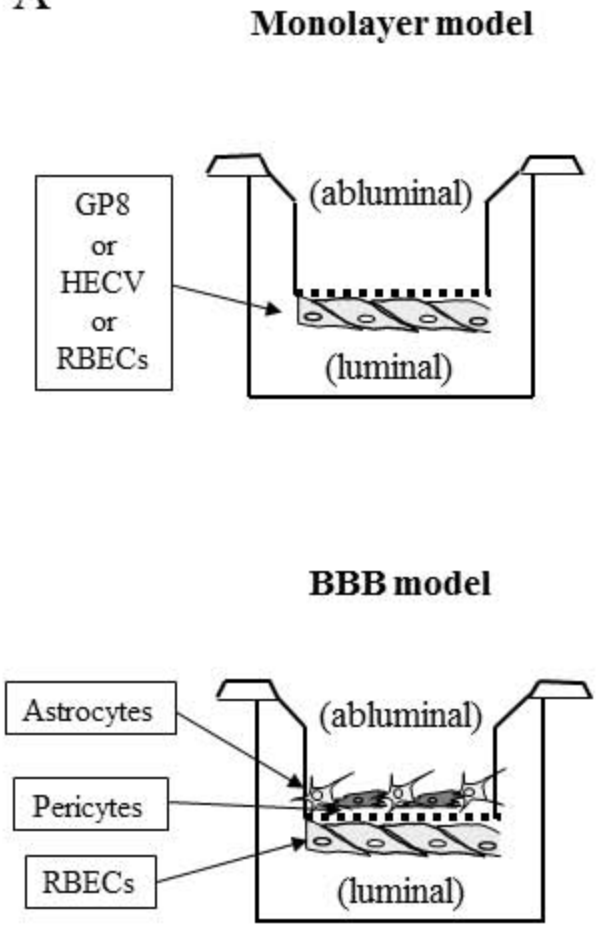
Monolayer model
GP8
or
HECV
or
RBECs
(abluminal)
(luminal)
BBB model
Astrocytes
Pericytes
RBECs
(abluminal)
(luminal)

B

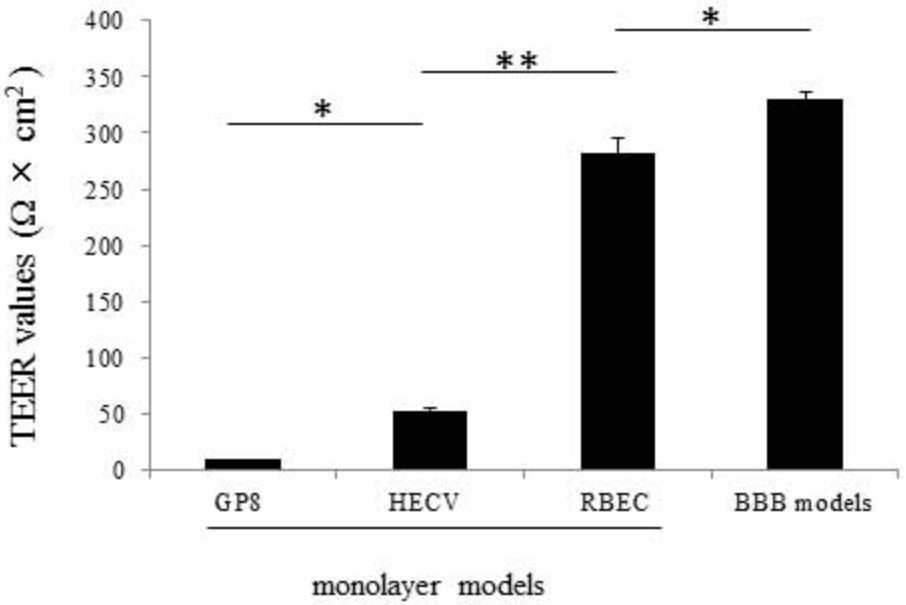
TEER values (Ω × cm²)
400
350
300
250
200
150
100
50
0
*
**
*
GP8
HECV
RBEC
BBB models
monolayer models

Fig. 2

A

Fibronectin-coated membrane

0.4 μm pores

8 μm pores

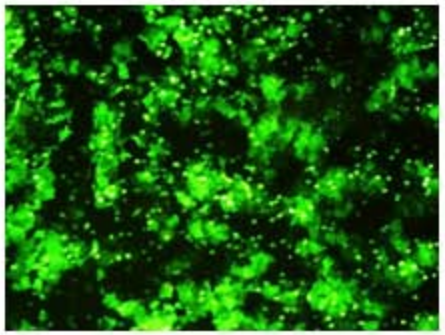

B

Cell monolayer models with 8 μm pore-sized membrane

GP8

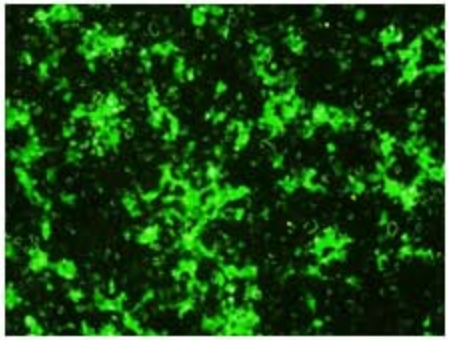

HECV

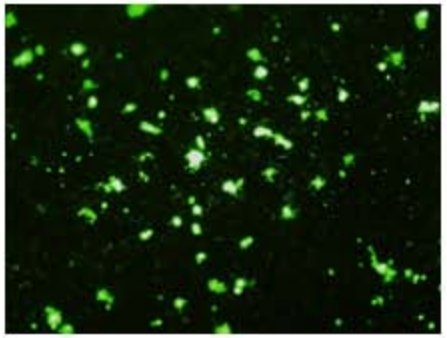

RBEC

Fig. 3

A

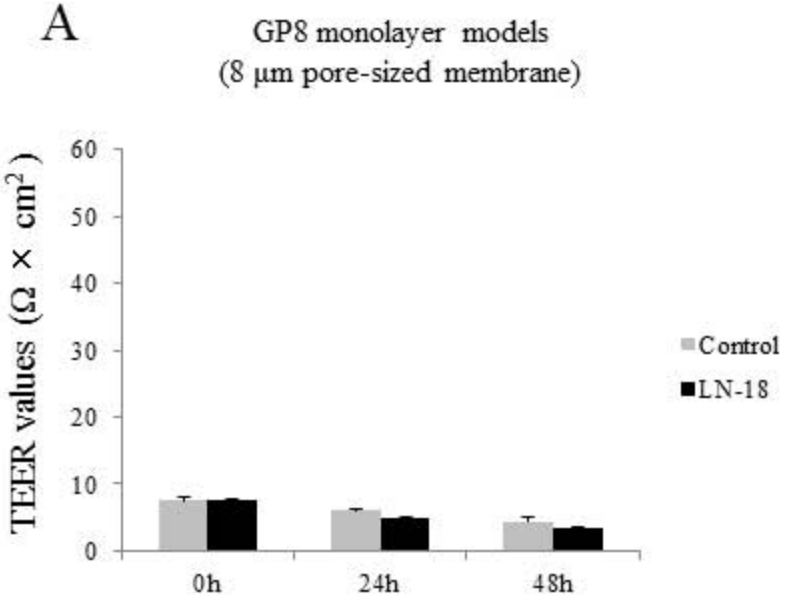
GP8 monolayer models
(8 μm pore-sized membrane)
TEER values (Ω × cm²)
60
50
40
30
20
10
0
0h
24h
48h
Control
LN-18

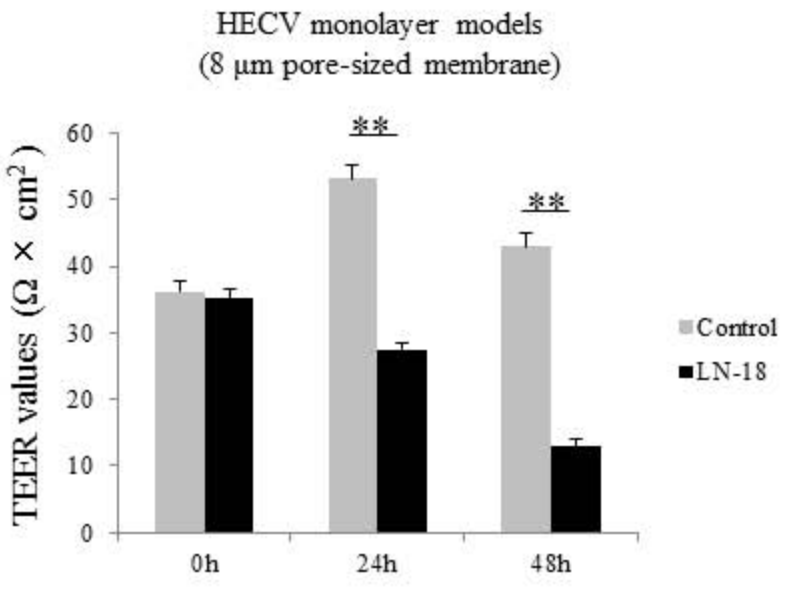
HECV monolayer models
(8 μm pore-sized membrane)
TEER values (Ω × cm²)
60
50
40
30
20
10
0
**
**
0h
24h
48h
Control
LN-18

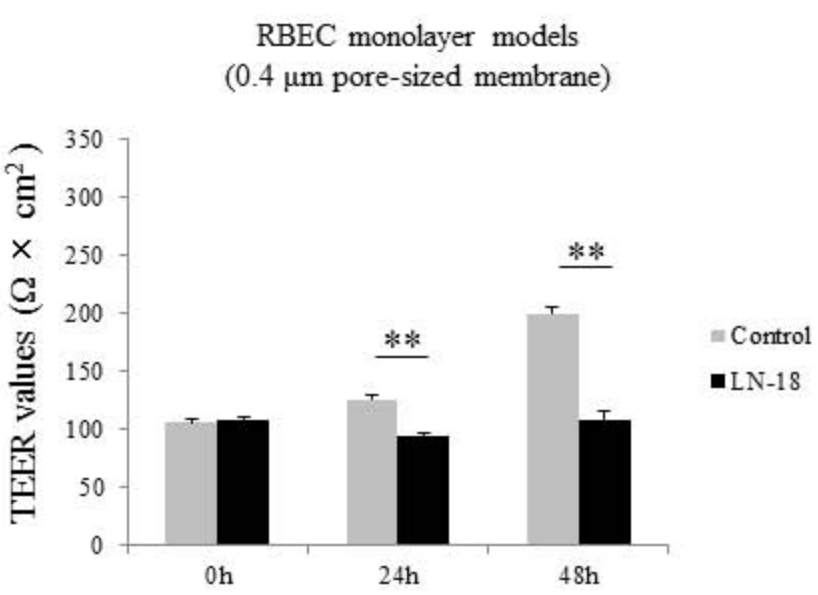
RBEC monolayer models
(0.4 μm pore-sized membrane)
TEER values (Ω × cm²)
350
300
250
200
150
100
50
0
**
**
0h
24h
48h
Control
LN-18

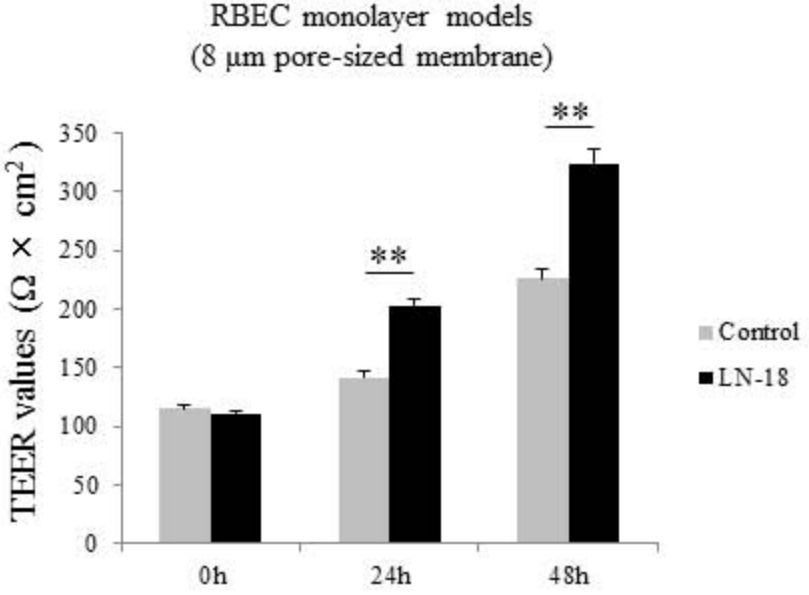
RBEC monolayer models
(8 μm pore-sized membrane)
TEER values (Ω × cm²)
350
300
250
200
150
100
50
0
**
**
0h
24h
48h
Control
LN-18

Fig. 3

B

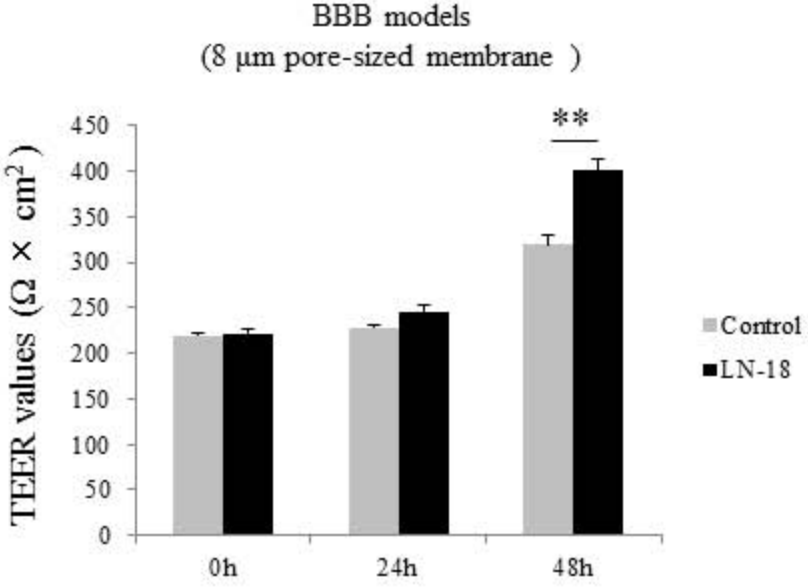

Lower surface of the membrane
after 10 days from LN-18-GFP cells
application into BBB model

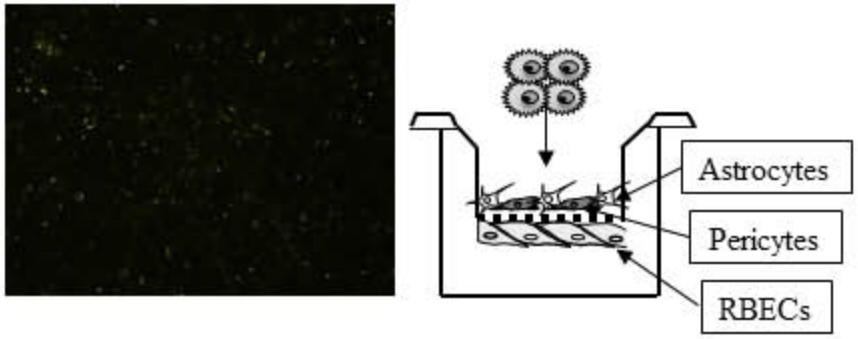

Lower surface of the membrane
after 48 hours from LN-18-GFP cells application
into pericytes/astrocytes monolayer model

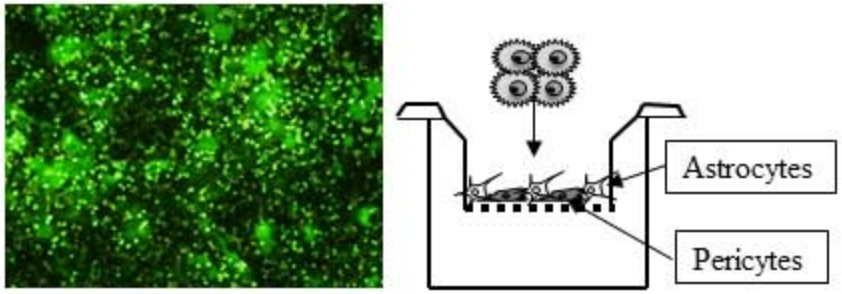

Fig. 4

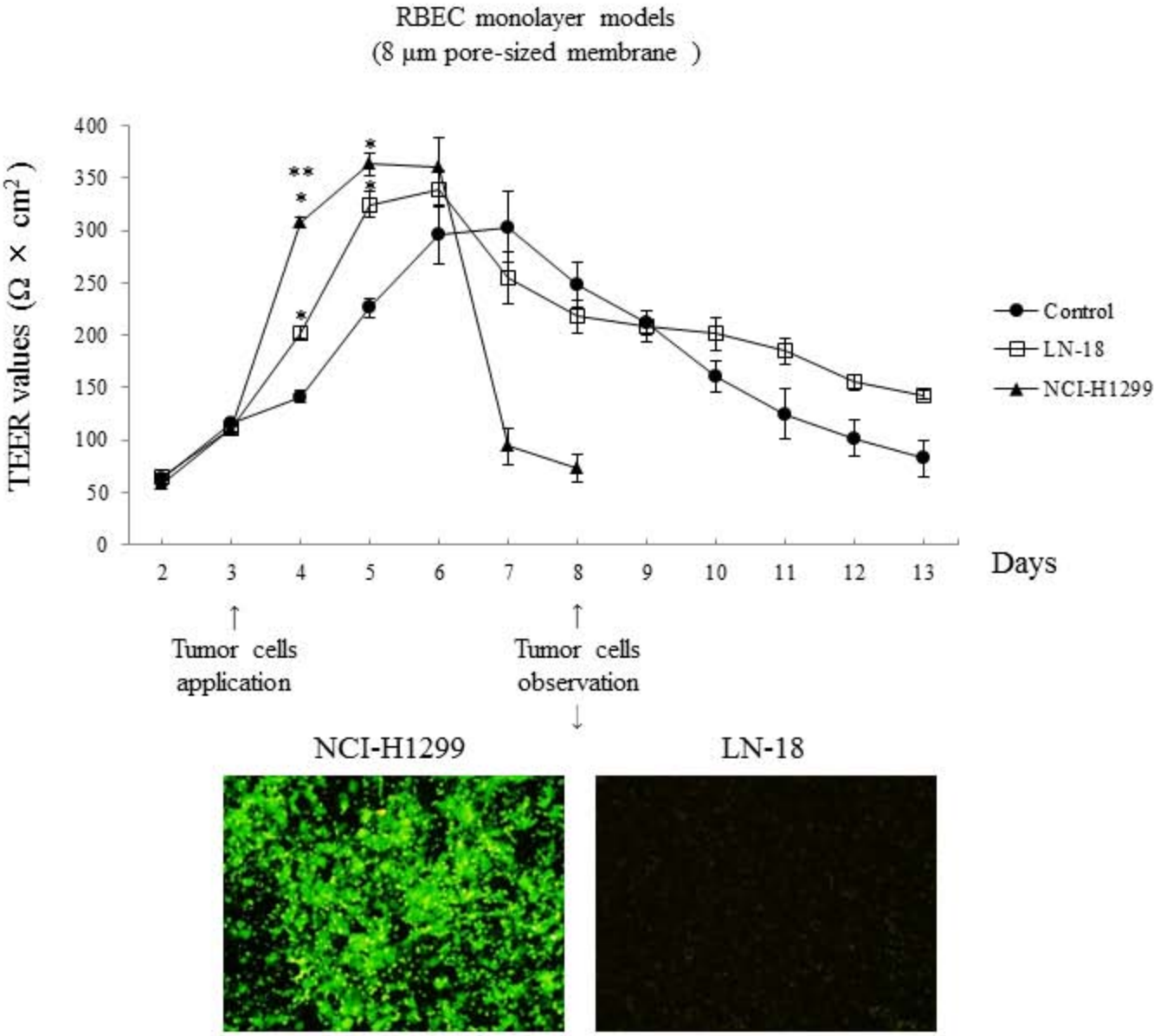
RBEC monolayer models
(8 μm pore-sized membrane)
TEER values (Ω × cm²)
400
350
300
250
200
150
100
50
0
2
3
4
5
6
7
8
9
10
11
12
13
Days
Control
LN-18
NCI-H1299
Tumor cells application
Tumor cells observation
NCI-H1299
LN-18

Fig. 5

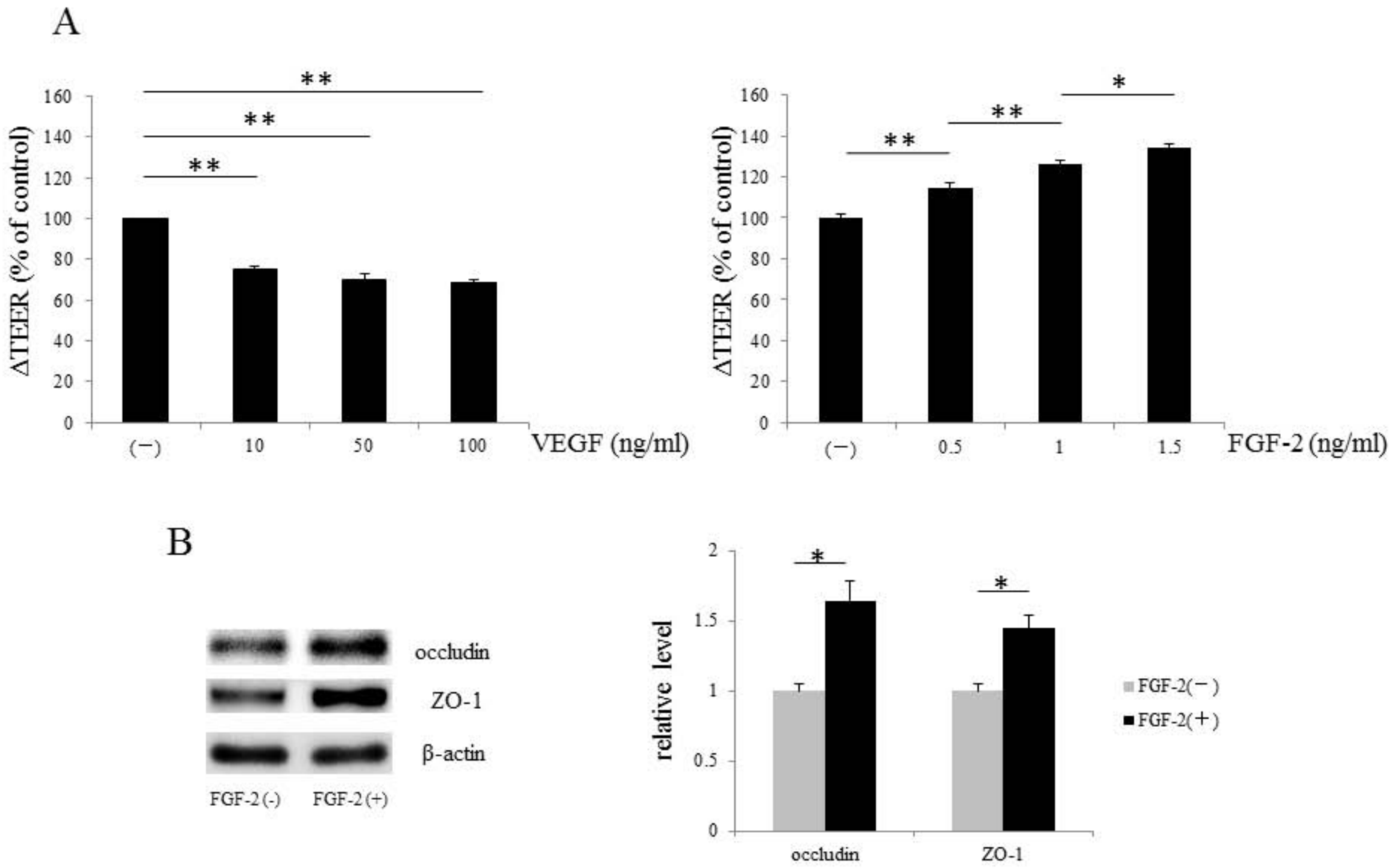
A
ΔTEER (% of control)
160
140
120
100
80
60
40
20
0
**
**
**
(−)
10
50
100
VEGF (ng/ml)
ΔTEER (% of control)
160
140
120
100
80
60
40
20
0
**
**
*
(−)
0.5
1
1.5
FGF-2 (ng/ml)
B
occludin
ZO-1
β-actin
FGF-2 (-)
FGF-2 (+)
relative level
2
1.5
1
0.5
0
*
*
occludin
ZO-1
FGF-2(−)
FGF-2(+)

Fig. 6


Control
ΔTEER (% of control)
120
100
80
60
40
20
0
0h
6h
LN-18
**
ΔTEER (% of control)
120
100
80
60
40
20
0
0h
6h

Table 1
VEGF and FGF-2 secretion by GBM and lung cancer cells in conditioned media

	Control media	LN-18-CM	U-87 MG-CM	NCI-H1299-CM
VEGF (pg/ml)	0.00	3,499.8 ± 78.5	4,933.6 ± 169.7	2,495.2 ± 26.5
FGF-2 (pg/ml)	0.00	10.8 ± 0.6	6.3 ± 0.2	30.2 ± 0.3

LN-18-GFP , U-87 MG , and NCI-H1299-GFP cells were grown in the 10 cm dishes and the conditioned media were harvested after 72 h. The amounts of VEGF or FGF-2 in the conditioned media were measured using enzyme-linked immunosorbent assay. VEGF or FGF-2 levels in the conditioned media without any cells were also measured as a control value